Electronic Supplementary Material (ESI) for Physical Chemistry Chemical Physics.

Supplementary Information

Reaction Mechanism and Electronic Properties of Host-Guest Energetic Materials CL-20/HA under High Pressure by Quantum-Based Molecular Dynamics Simulations

Yiwen Xiao, Lang Chen, Kun Yang, Jianying Lu, Junying Wu*

State Key Laboratory of Explosion Science and Technology, Beijing Institute of Technology, Beijing 100081, China

Corresponding Author: Lang Chen, Tel: +86 10 68914711.

E-mail: chenlang@bit.edu.cn

Table of contents

Table S1. Lattice parameters of optimized CL-20/HA

	Original	Optimized	Error
a/Å	19.577	19.609	0.16%
b/Å	13.123	13.117	0.05%
c/Å	23.509	23.546	0.16%

The convergence criterion for the maximum geometry change between the current and the last optimizer iteration was $<3.0\times10^{-3}$ bohr. The root mean square (RMS) geometry change between the current and the last optimizer iteration was $<1.5\times10^{-3}$ bohr. The maximum force component was $<4.5\times10^{-4}$ hartree/bohr. The RMS force was $<3.0\times10^{-4}$ hartree/bohr. The residual pressure was <100 Pa. The optimized lattice parameters were basically consistent with the original parameters, and the maximum error was less than 1%. The angle of the orthorhombic cell in the three directions was all 90°. The maximum deviation after optimization was γ=90.031°. The optimized cell was feasible for subsequent calculations.

The change in total energy per atom is already less than 2E-6 eV/atom when the energy cutoff is greater than 400 Ry, as shown in Figure S1. Therefore, we believe that this cutoff value is reasonable.

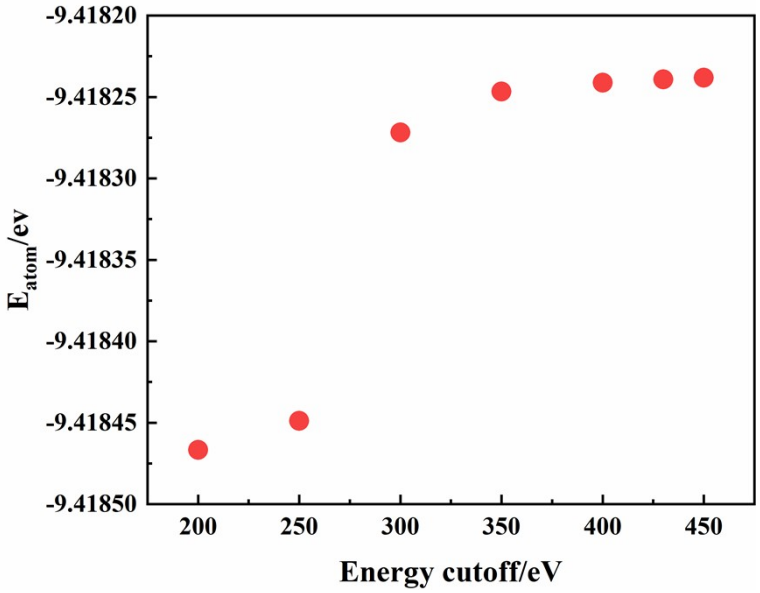

Figure S1. Change of total energy per atom with energy cutoff.

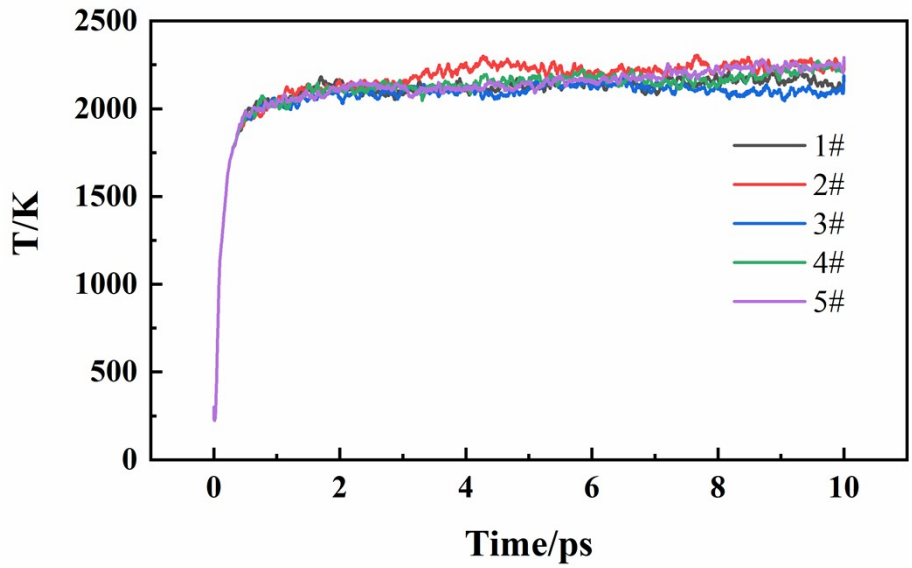

(a)

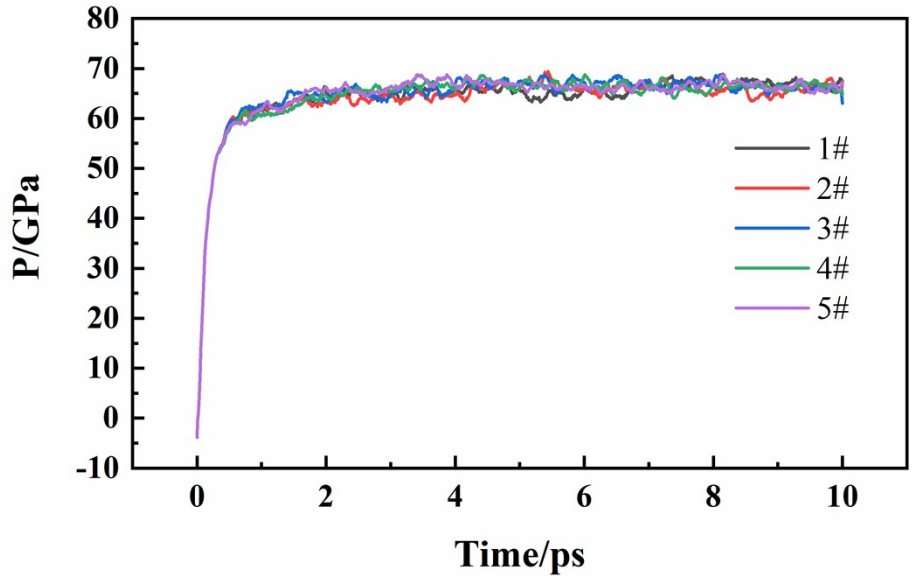

(b)

Figure S2. Evolution of average temperature (a) and pressure (b) of the CL-20/HA system at 9 km/s shock velocity along the a [100] direction in five independent simulations. The evolution of thermodynamic parameters T and P are very similar in the repetitive simulations. The fluctuation is within reasonable limits.

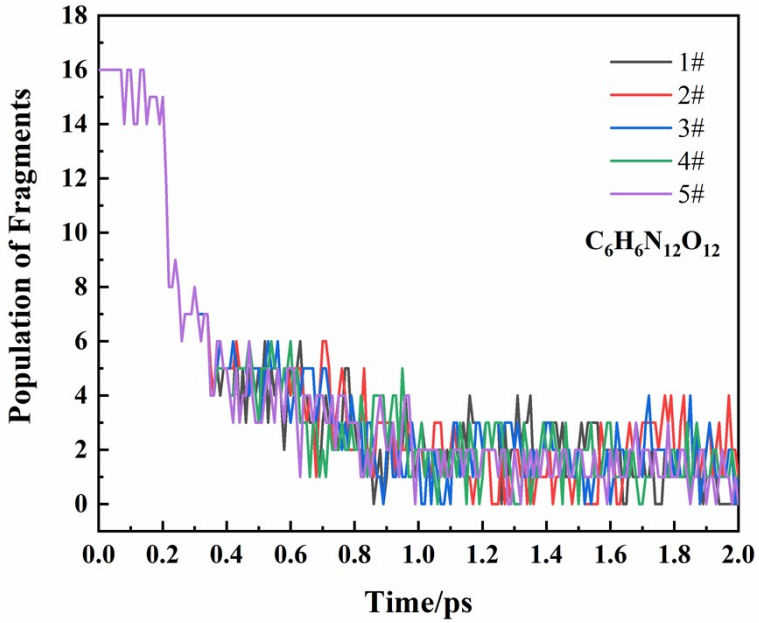

Figure S3. Evolution of the population of $C_6H_6N_{12}O_{12}$ molecules with time in five independent simulations. The decomposition of reactant CL-20.

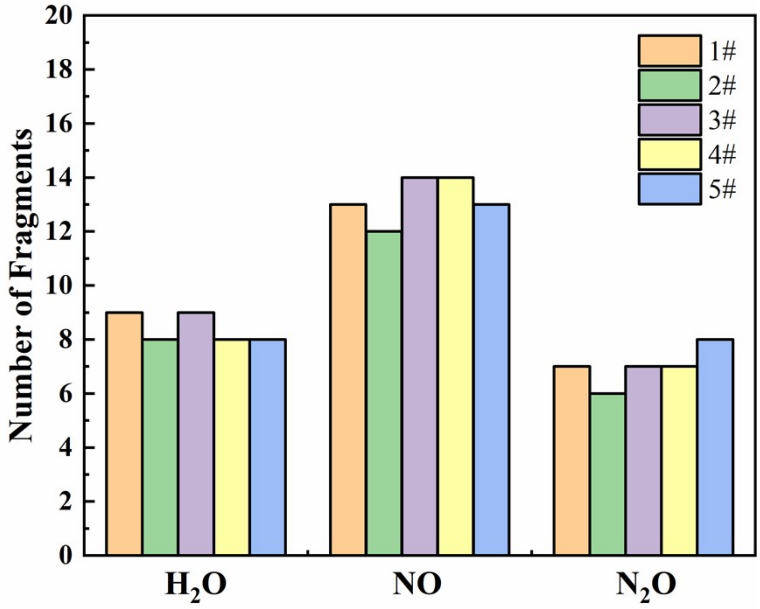

Figure R4. Number of H_2O, NO, and N_2O small molecular products at 10 ps in five independent simulations. The generation of products.

The change in the number of $C_6H_6N_{12}O_{12}$ molecules before ~0.4 ps in five times repetitive simulations is exactly the same. Differences appeared in the later time, by then most of the $C_6H_6N_{12}O_{12}$ molecules had already reacted. This indicates that the initial reaction path of CL-20 is likely to be the same in each simulation. The number of main small molecular products

at 10 ps is close in five times repetitive simulations. The average difference is just about 1.

All calculations were performed on the same cluster server with the same settings to ensure maximum consistency.

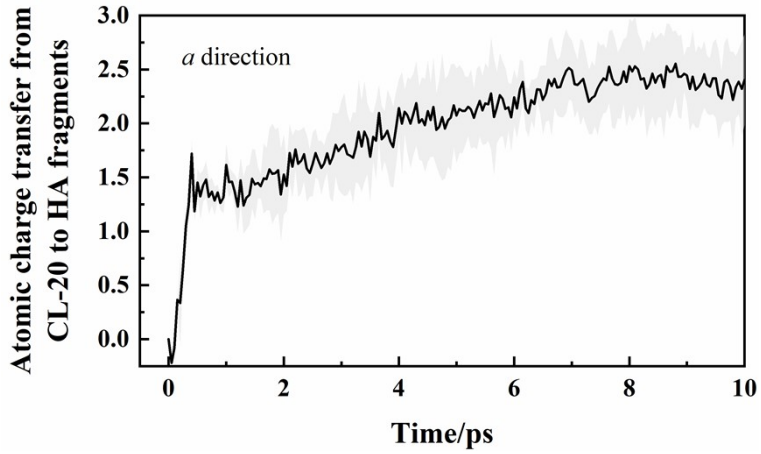

(a)

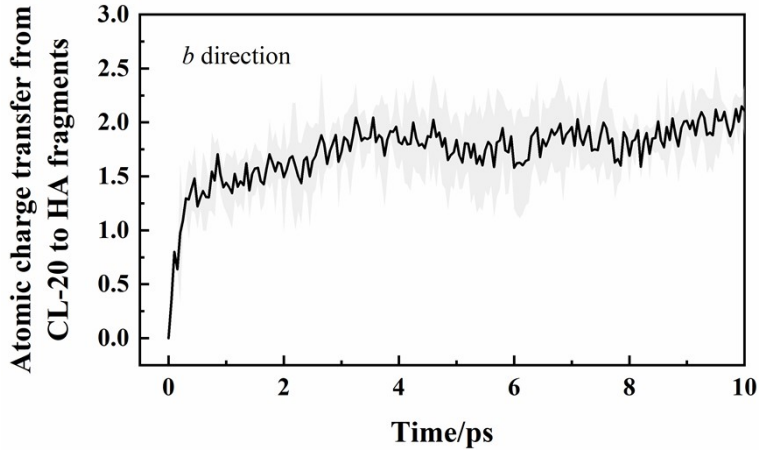

(b)

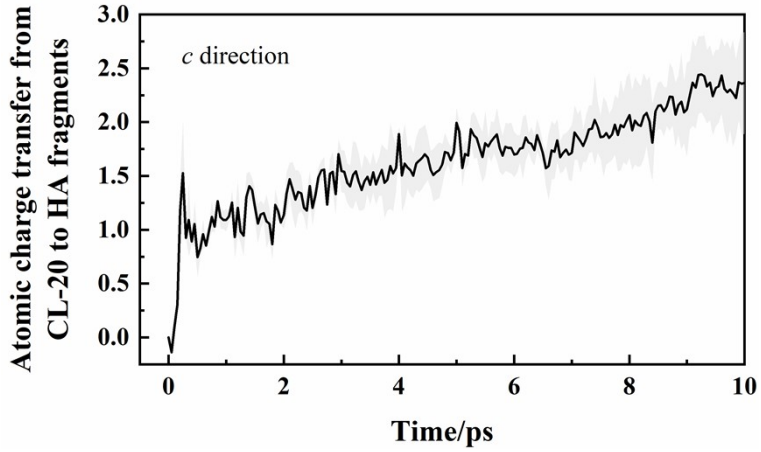

(c)

Figure S5. Changes of the total charge transfer from the CL-20 molecules to HA molecules at 9 km/s along the different directions. The curves are surrounded by error bands.

The directional charge transfer is observed in all directions. The system is no longer in a local charge equilibrium state under shock loading.

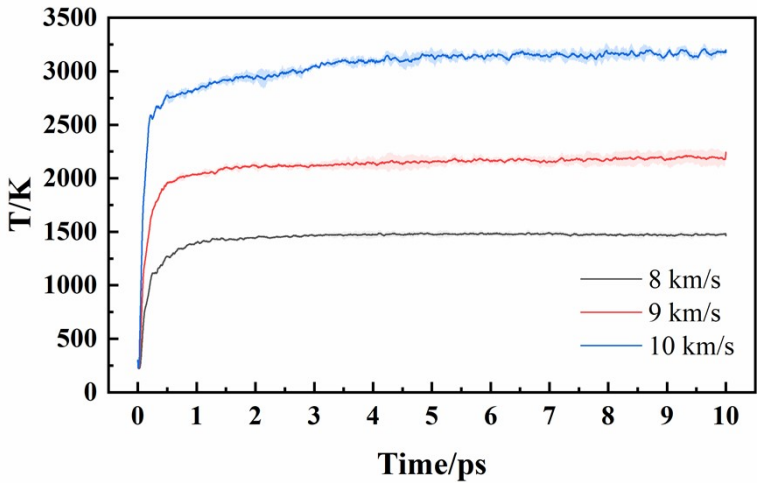

(a)

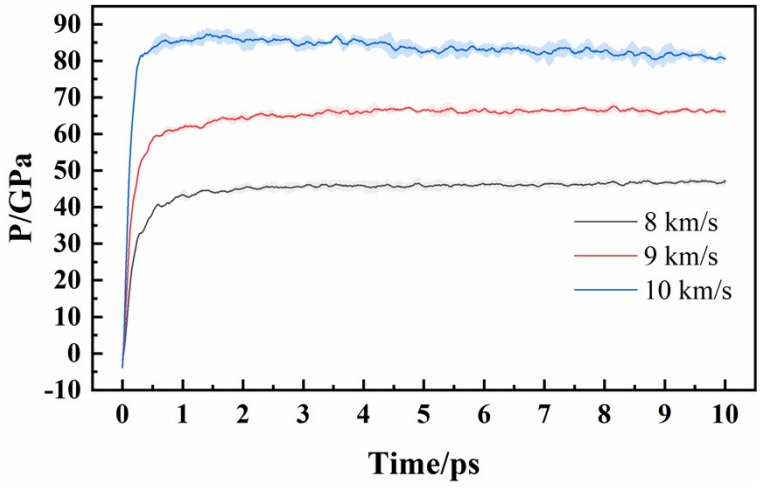

(b)

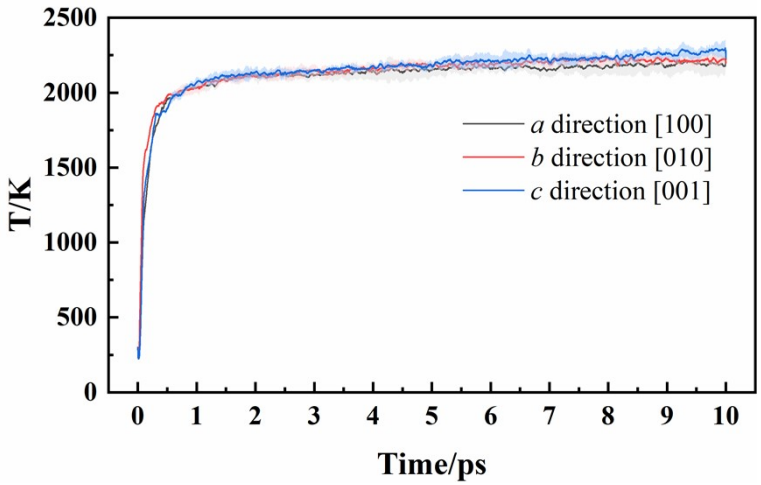

(c)

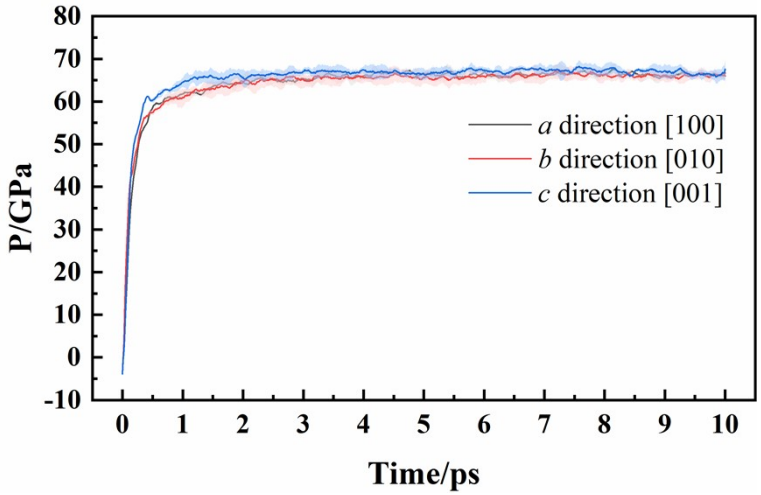

(d)

Figure S6. Evolution of average temperature (a) and pressure (b) of the CL-20/HA with time at different shock velocities along the *a* directions. Evolution of average temperature (c) and pressure (d) with time at 9 km/s along the different directions.

The volume of the calculation system is compressed sharply under the loading of shock wave with different velocities. The temperature and pressure also increase rapidly. The greater the shock velocity, the greater the maximum temperature and pressure. At the same shock velocity of 9 km/s, the temperature and the pressure values of different directions are similar.

The first excitation stage lasts for about 0.4 ps at shock velocity of 9 km/s. Then the temperature and pressure of the system almost reach a peak, which marks the onset of the violent reaction stage.

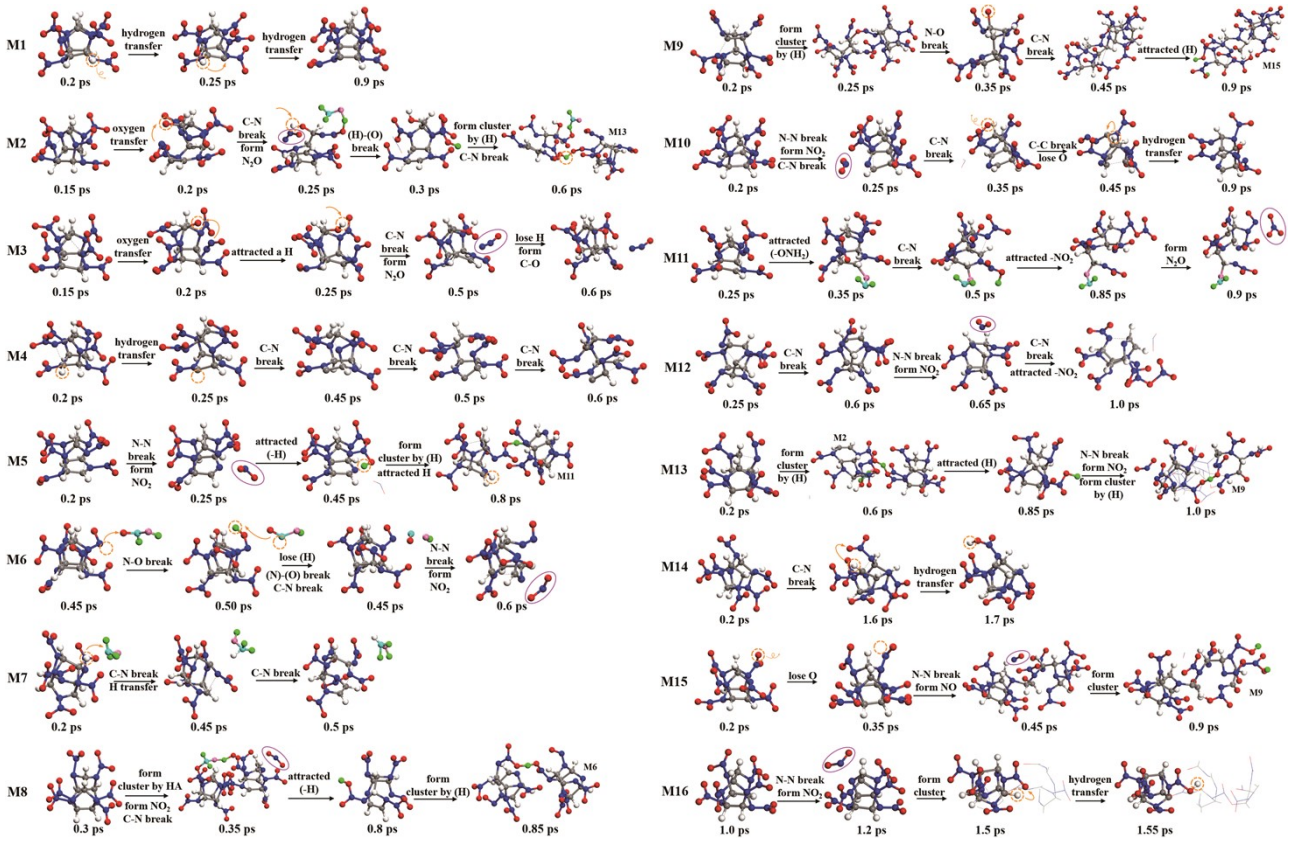

Figure S7. Snapshots of the initial reaction paths of the CL-20/HA at shock velocity of 9 km/s.

The destruction of cage structure in CL-20 occurs first under shock, as molecule M1, M2 and M3. The cage structure absorbs the energy of the shock wave. Free NO_2 generated by N–NO_2 cleavage is also observed earlier, such as M5, M8, M10.

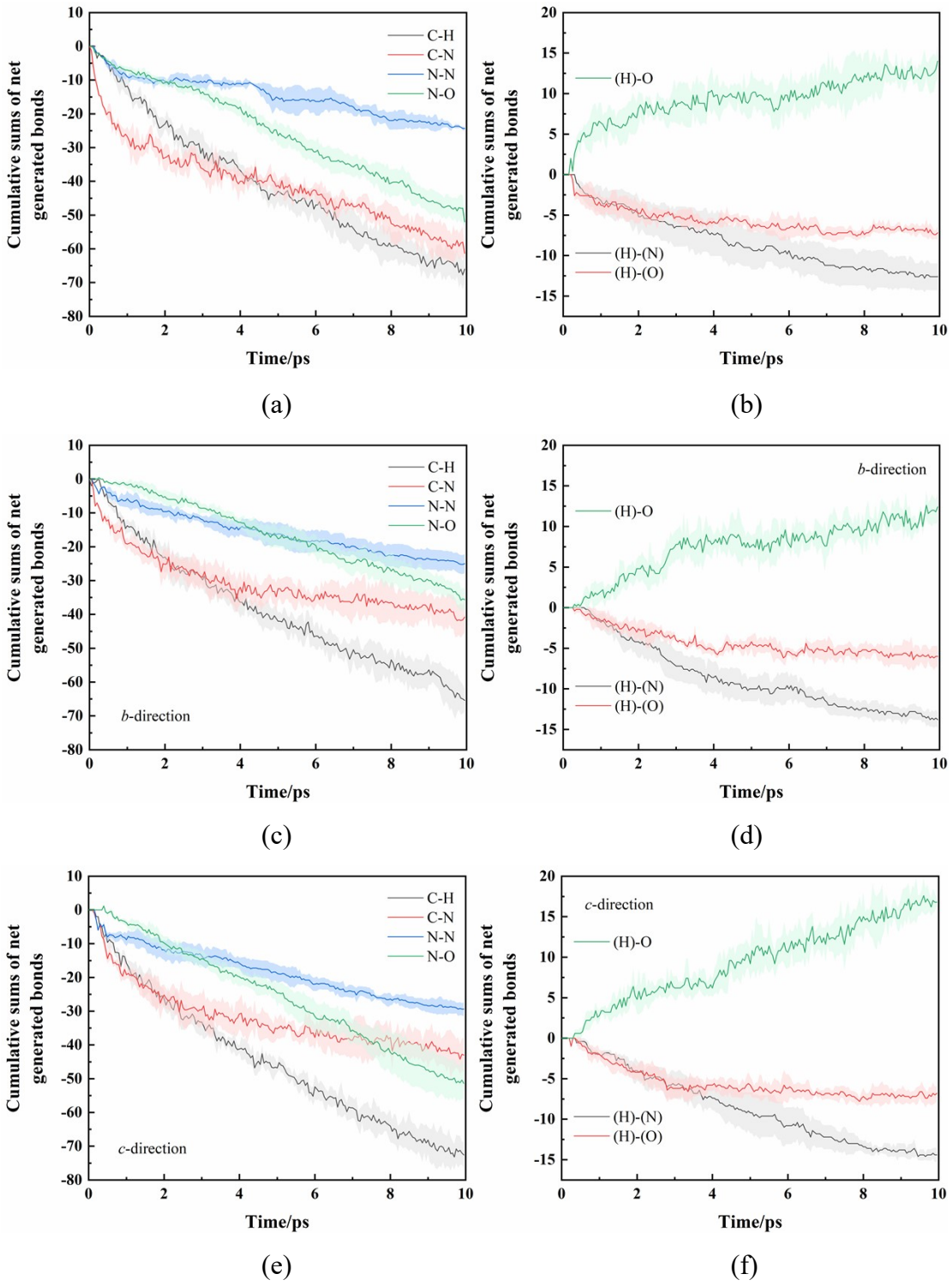

Figure S8. Cumulative sums of net generated bonds between (H), (O) atoms form HA and C, H, N, and O atoms from CL-20. (a), (c) and (e) represent the decomposition of CL-20 in *a*, *b,* and *c* directions. (b), (d) and (f) represent the decomposition of HA and the fastest way of HA participating in CL-20 reactions.

Positive values represent the generation of bonds. Negative values

represent the broken of bonds. The number of net generated (H)–(N) and (H)–(O) bonds decreases gradually at time zero, which means the decomposition of HA molecules. The other bonds have been increasing, among which (H)–O bonds is the largest. The findings show that HA molecules first break (H)–(N) and (H)–(O) bonds to form free H atoms. These free H atoms are easy to bond with O atoms in CL-20 nitro group.

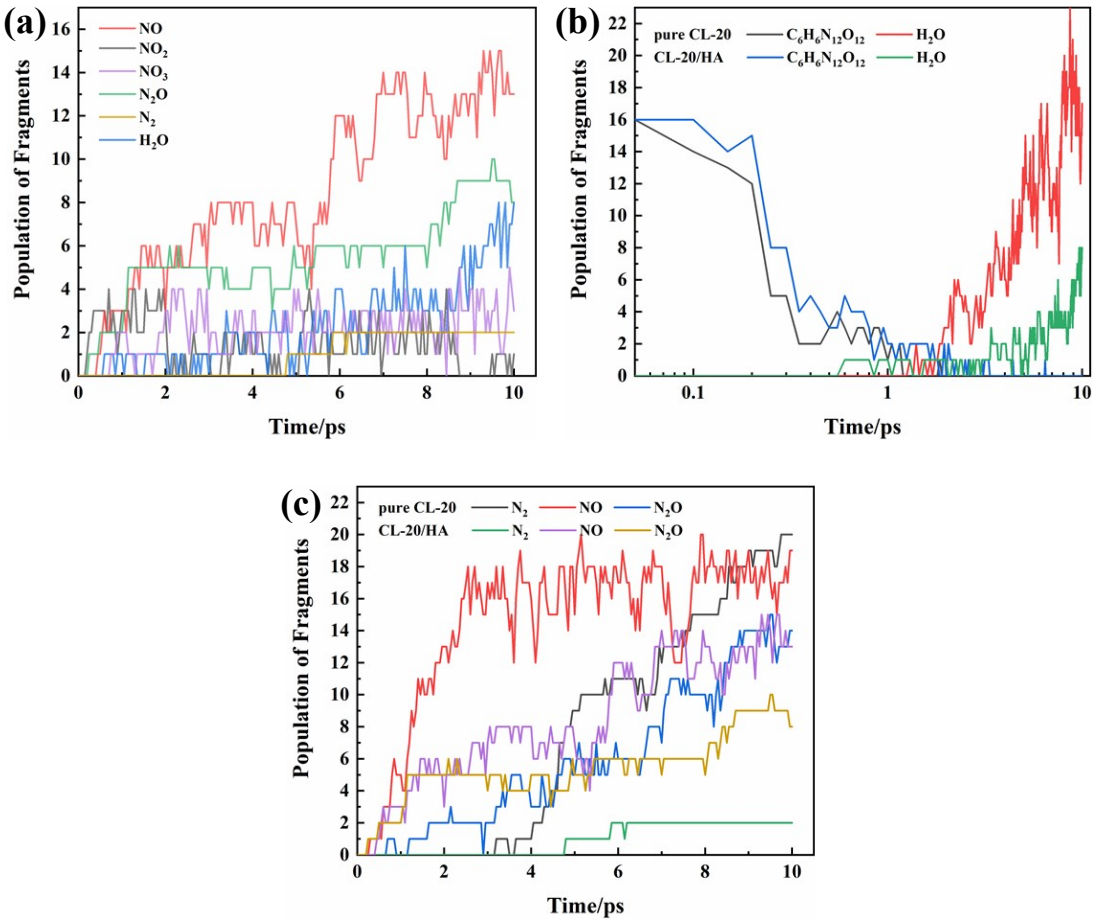

Figure S9. (a) Evolution of the population of intermediate small molecules with time in the CL-20/HA. Evolution of (b) $C_6H_6N_{12}O_{12}$ and H_2O, (c) N_2, NO and N_2O molecules with time in the CL-20/HA and pure CL-20 system respectively.

The decline rate of CL-20, the generation rate and number of small molecular products H_2O, N_2, and NO in CL-20/HA system are less than those in pure CL-20 system. The number of N_2O in pure CL-20 system is small at the beginning, after about 3.5 ps, it exceeds that of CL-20/HA system and gradually increases all the time.